Published in final edited form as:
Diabetes. 2005 December ; 54(12): 3435–3441.

Oxidative-Nitrosative Stress and Poly(ADP-Ribose) Polymerase (PARP) Activation in Experimental Diabetic Neuropathy:

The Relation Is Revisited

Irina G. Obrosova[1,2], **Viktor R. Drel**[1], **Pal Pacher**[3], **Olga Ilnytska**[1], **Zhong Q. Wang**[1], **Martin J. Stevens**[2], and **Mark A. Yorek**[4]

[1]*Pennington Biomedical Research Center, Louisiana State University System, Baton Rouge, Louisiana* [2]*Department of Internal Medicine, University of Michigan, Ann Arbor, Michigan* [3]*Laboratory of Physiological Studies, National Institutes of Health/National Institute of Alcohol Abuse and Alcoholism, Bethesda, Maryland* [4]*Veteran Affairs Medical Center and Department of Internal Medicine, University of Iowa, Iowa City, Iowa*

Abstract

Poly(ADP-ribose) polymerase (PARP) activation, an important factor in the pathogenesis of diabetes complications, is considered a downstream effector of oxidative-nitrosative stress. However, some recent findings suggest that it is not necessarily the case and that PARP activation may precede and contribute to free radical and oxidant-induced injury. This study evaluated the effect of PARP inhibition on oxidative-nitrosative stress in diabetic peripheral nerve, vasa nervorum, aorta, and high glucose–exposed human Schwann cells. In vivo experiments were performed in control rats and streptozocin (STZ)-induced diabetic rats treated with and without the PARP inhibitor 3-aminobenzamide (ABA) (30 mg · kg^{-1} · day^{-1} i.p. for 2 weeks after 2 weeks of untreated diabetes). Human Schwann cells (HSC) (passages 7–10; ScienCell Research Labs) were cultured in 5.5 or 30 mmol/l glucose with and without 5 mmol/l ABA. Diabetes-induced increase in peripheral nerve nitrotyrosine immunoreactivity, epineurial vessel superoxide and nitrotyrosine immunoreactivities, and aortic superoxide production was reduced by ABA. PARP-1 (Western blot analysis) was abundantly expressed in HSC, and its expression was not affected by high glucose or ABA treatment. High-glucose–induced superoxide production and overexpression of nitrosylated and poly(ADP-ribosyl)ated protein, chemically reduced amino acid-(4)-hydroxynonenal adducts, and inducible nitric oxide synthase were decreased by ABA. We concluded that PARP activation contributes to superoxide anion radical and peroxynitrite formation in peripheral nerve, vasa nervorum, and aorta of STZ-induced diabetic rats and high-glucose–exposed HSC. The relations between oxidative-nitrosative stress and PARP activation in diabetes are bi-rather than unidirectional, and PARP activation cannot only result from but also lead to free radical and oxidant generation.

Oxidative-nitrosative stress produced by free radicals and oxidants contributes to nerve conduction deficits (1–3), metabolic changes (3,4), impaired neurotrophic support (5), neurovascular dysfunction (1,2), abnormal sensation, and pain (6,7), as well as morphological abnormalities (8) characteristic for peripheral diabetic neuropathy (PDN). Enhanced oxidative-nitrosative stress is manifest in peripheral nerve, dorsal root and sympathetic ganglia, and vasculature of the peripheral nervous system of animals with both type 1 and type 2 diabetes (1,3,9–13). One of the important, currently considered as downstream, effectors of oxidative-nitrosative injury and associated DNA single-strand breakage is activation of the nuclear

Address correspondence and reprint requests to Irina G.Obrosova, PhD, Pennington Biomedical Research Center, Louisiana State University, 6400 Perkins Rd., Baton Rouge, LA 70808. E-mail: obrosoig@pbrc.edu.

enzyme poly(ADP-ribose) polymerase (PARP). Once activated, PARP cleaves nicotinamide adenine dinucleotide (NAD^+) with formation of nicotinamide and ADP-ribose residues, which are attached to nuclear proteins with formation of poly(ADP-ribosyl)ated protein polymers. The process leads to *1*) NAD^+ depletion and energy failure (16,17), *2*) changes of transcriptional regulation and gene expression (18), and *3*) poly(ADP-ribosyl)ation and inhibition of glyceraldehyde 3-phosphate dehydrogenase resulting in diversion of the glycolytic flux toward several pathways implicated in diabetes complications (19). Growing evidence suggests that PARP activation represents a fundamental step in the pathogenesis of diabetes complications (16,17,20–23). Our group has recently demonstrated the important role of PARP in nerve conduction deficits, neurovascular dysfunction, and energy failure, as well as thermal and mechanical hyperalgesia in early PDN (17,23).

The interactions between oxidative-nitrosative stress and PARP are complex, and recent observations do not support the premise that PARP activation is a mere consequence of free radical and oxidant-induced damage. On the one hand, PARP activation in bovine aortic endothelial cells was documented within 2 h of exposure to high glucose (19), i.e., at the time when neither enhanced dichlorofluorescein fluorescence (an index of intracellular oxidative stress) nor accumulation of nitrosylated proteins in these particular cells and conditions are detectable (I.G.O., M.J.S., V.R.D., unpublished observations). Furthermore, PARP activation, but not DNA single-strand breakage, was identified in dorsal root ganglia neurons of streptozocin (STZ)-induced diabetic rats (10), whereas in the retina, poly(ADP-ribosyl)ated proteins accumulated both in the cells containing DNA breaks and in those with preserved DNA integrity (T.S. Kern, personal communication). This suggests that some unidentified, potentially metabolic, mechanism(s) of PARP activation, different from oxidative-nitrosative stress, may operate in diabetic and hyperglycemic conditions. On the other hand, PARP activation affects glucose utilization, transcriptional regulation, and gene expression and thus can potentially contribute to oxidative-nitrosative stress via multiple mechanisms. Our animal and cell culture studies provide the first evidence of the major contribution of PARP activation to oxidative-nitrosative stress in peripheral nerve, vasa nervorum, and aorta of STZ-induced diabetic rats, as well as high-glucose–exposed human Schwann cells (HSC).

RESEARCH DESIGN AND METHODS

Unless otherwise stated, all chemicals were of reagent-grade quality and were purchased from Sigma Chemical, St. Louis, MO. Reagents for immunohistochemistry have been purchased from Vector Laboratories, Burlingdale, CA, and Dako Laboratories, Santa Barbara, CA. HSC and HSC medium were purchased from ScienCell Research Laboratories, San Diego, CA.

The experiments were performed in accordance with regulations specified by the National Institutes of Health 1985 Principles of Laboratory Animal Care and University of Michigan Protocol for Animal Studies. Male Wistar rats (Charles River, Wilmington, MA), body weight 250–300 g, were fed a standard rat diet (PMI Nutrition, Brentwood, MO) and had access to water ad libitum. STZ-induced diabetes was induced as described (4,11,16,17). Blood samples for glucose measurements were taken from the tail vein ~48 h after the STZ injection and the day before the animals were killed. The rats with blood glucose ≥13.8 mmol/l were considered to have diabetes. The experimental groups were comprised of control rats and diabetic rats treated with and without the PARP inhibitor 3-aminobenzamide (ABA) (30 $mg \cdot kg^{-1} \cdot day^{-1}$ i.p.). The treatments were started 2 weeks after the initial 2 weeks without treatment. We have previously reported that STZ-induced diabetic rats with short-term (4- to 6-week) duration of diabetes had clearly manifest oxidative-nitrosative stress and PARP activation in the peripheral nerve (11,17,24) and, therefore, are quite suitable for mechanistic studies of interactions between the two phenomena. Furthermore, in an earlier study with an identical experimental design we found that ABA, at the aforementioned dose, corrected motor and

sensory nerve conduction deficits (motor nerve conduction velocity [m/s]: controls: 58.1 ± 1.8, controls + ABA: 58.9 ± 1.5, diabetes: 43.7 ± 1.4 [$P < 0.01$ vs. controls], diabetes + ABA: 56.2 ± 1.9 [$P < 0.01$ vs. untreated diabetes] and sensory nerve conduction velocity [m/s]: controls: 39.4 ± 1.6, controls +ABA: 38.7 ± 1.0, diabetes: 30.2 ± 0.5 [$P < 0.01$ vs controls], diabetes + ABA: 36.1 ± 0.6 [$P < 0.01$ vs. untreated diabetes]), as well as neurovascular dysfunction and energy failure in STZ-induced diabetic rats (17).

Anesthesia, euthanasia, and tissue sampling

The animals were sedated by CO_2 (24) and immediately killed by cervical dislocation. Both sciatic nerves were rapidly dissected and fixed in formalin (17) for assessment of nitrotyrosine and poly(ADP-ribose) by immunohistochemistry. Some sciatic nerves were used for isolation of epineurial arterioles (1) and assessment of arteriolar superoxide anion radical and nitrotyrosine. Aortas have also been sampled and immediately used for superoxide measurements.

HSC culture

HSC were cultured in commercial media, according to manufacturer's instructions. Passages 7–10 were used in all experiments.

Specific methods

Immunohistochemical studies—All sections were processed and evaluated blindly.

NT immunoreactivity—Nitrotyrosine immunoreactivity was assessed as described (11). The intensity of staining was graded from 1 to 4 (1, no staining; 2, faint; 3, moderate; and 4, intense), and the immunohistochemistry score was expressed as mean ± SE for each experimental group. Similar staining procedure has been used for epineurial vessel sections.

Poly(ADP-ribose) immunoreactivity—Poly(ADP-ribose) immunoreactivity was assessed as described (17). The number of poly(ADP-ribose)-positive nuclei were calculated for each microphotograph.

Superoxide in epineurial vessels and aorta—Superoxide anion radical abundance in epineurial vessels was assessed by the hydroethidine method as described (1). The intensity of superoxide fluorescence was graded from 1 to 4 (1, no fluorescence; 2, weak; 3, moderate; and 4, intense), and the immunohistochemistry score was expressed as mean ± SE for each experimental group. Superoxide anion radical abundance in aorta was measured by lucigenin-enhanced chemiluminescence (1).

Superoxide in HSC—HSC were cultured in 6-well plates in media containing either 5.5 or 30 mmol/l glucose with and without ABA, 5 mmol/l, or the potent, cell permeable superoxide dismutase mimetic Mn(III)TBAP, 50 μmol/l (Cayman Chemical, Ann Arbor, MI). Mn(III) TBAP was used as a positive control. Culture media were then aspirated and the cells washed with PBS. Two milliliters of serum-free medium containing 50 μl of 10 μmol/l hydroethidine (Molecular Probes) was added per well at 37°C for 30 min. Then the cells were washed with PBS and trypsinized, and the ethidium fluorescence (an index of superoxide generation) was measured by spectrofluorometry (LS 55 Luminescence Spectrometer [Perkin Elmer], λ excitation 465 nm, λ emission 630 nm). After spectrofluorometry, the cells were counted, and fluorescence was expressed per 10^4 cells.

Western blot analysis—HSC were cultured for 24 h in media containing either 5.5 mmol/l or 30 mmol/l glucose with and without 5 mmol/l ABA. Western blot analysis of cell lysates

(100 μg) was performed as described (23,25), with nitrotyrosine, poly(ADP-ribose), PARP-1 (Biomol, Plymouth Meeting, PA), inducible nitric oxide synthase (iNOS) (Santa Cruz, Santa Cruz, CA), or chemically reduced amino acid-(4)-hydroxynonenal adduct (hydroxynonenal [HNE] adduct; Calbiochem) antibodies. Total content of all nitrosylated and poly(ADP-ribosyl)ated proteins and HNE adducts as well as iNOS and PARP-1 was quantified by densitometry (Quantity One 4.5.0 software; Bio-Rad Laboratories, Richmond, CA). Membranes were then stripped in the 62.5 mmol/l Tris-HCl, pH 6.7, buffer containing 2% SDS and 100 mmol/lβ-mercaptoethanol and reprobed with β-actin antibody to confirm equal protein loading.

Statistical analysis

The results are expressed as means ± SE. Data were subjected to equality of variance *F* test and then to log transformation, if necessary, before one-way ANOVA. Where overall significance ($P < 0.05$) was attained, individual between-group comparisons were made using the Student-Newman-Keuls multiple range test. Significance was defined at $P < 0.05$. When between-group variance differences could not be normalized by log transformation (datasets for body weights and plasma glucose), the data were analyzed by the nonparametric Kruskal-Wallis one-way ANOVA, followed by the Bonferroni/Dunn test for multiple comparisons.

RESULTS

The final body weights were comparably lower in untreated and ABA-treated diabetic rats than in the control group (Table 1). The final blood glucose concentrations were similarly elevated in untreated and ABA-treated diabetic rats compared with the control rats.

Nitrotyrosine immunoreactivities were increased 2.3-fold in the sciatic nerves of diabetic rats compared with control rats, and this increase was markedly reduced by ABA treatment (Fig. 1*A* and *B*).

Poly(ADP-ribose) immunoreactivities were increased in the sciatic nerves of diabetic rats compared with controls, and this increase was reduced by ABA treatment (Fig. 1*C*). The number of the sciatic nerve poly(ADP-ribose)-positive nuclei was 2.7-fold greater in the diabetic group compared with the control group ($P < 0.01$, Fig. 1*D*). No significant differences in the numbers of sciatic nerve poly(ADP-ribose)-positive nuclei were found between the ABA-treated diabetic group and nondiabetic controls.

Ethidium fluorescence (an index of superoxide production) was increased ~2.8-fold in epineurial vessels of diabetic rats compared with controls (Fig. 2*A* and *B*), and this increase was blunted by ABA treatment. Nitrotyrosine immunoreactivity was increased threefold in epineurial vessels of diabetic rats, and this increase was reduced by ABA treatment (Fig. 2*C* and *D*).

Superoxide abundance in aorta was increased twofold in diabetic rats compared with control rats ($P < 0.01$, Fig. 3), and this increase was partially prevented by ABA treatment ($P < 0.01$ vs. untreated diabetic group).

Ethidium fluorescence was increased ~1.4-fold in HSC cultured in 30 mmol/l glucose compared with those cultured in 5.5 mmol/l glucose, and this increase was prevented by ABA and MnTBAP (Fig. 4). Neither ABA nor MnTBAP affected ethidium fluorescence in HSC cultured in 5.5 mmol/l glucose.

HNE adduct abundance was increased ~1.3-fold in HSC cultured in 30 mmol/l glucose compared with those cultured in 5.5 mmol/l glucose, and this increase was essentially (to 107%

of the control level) prevented by ABA (Fig. 5). ABA did not affect HNE adduct expression in HSC cultured in 5.5 mmol/l glucose.

iNOS expression was increased ~1.4-fold in HSC cultured in 30 mmol/l glucose compared with those cultured in 5.5 mmol/l glucose, and this increase was prevented by ABA. ABA did not affect iNOS expression in HSC cultured in 5.5 mmol/l glucose (Fig. 6).

Nitrosylated protein expression was increased 2.3-fold in HSC cultured in 30 mmol/l glucose compared with those cultured in 5.5 mmol/l glucose, and this increase was corrected by ABA (Fig. 7*A* and *B*). Poly(ADP-ribosyl)ated protein content was increased 1.8-fold in HSC cultured in 30 mmol/l glucose compared with those cultured in 5.5 mmol/l glucose, and this increase was prevented by ABA (Fig. 7*C* and *D*). PARP-1 was abundantly expressed in HSC, and this expression was not affected by high glucose or ABA treatment (Fig. 7*E* and *F*). ABA did not affect nitrosylated and poly(ADP-ribosyl)ated protein expression as well as PARP-1 expression in HSC cultured in 5.5 mmol/l glucose.

DISCUSSION

The PARP enzyme family consists of PARP-1 and several other poly(ADP-ribosyl)ating enzymes (26–28). The key role of reactive oxygen and nitrogen species and resulting DNA single-strand breakage in PARP activation is supported by *1*) in vitro demonstration of an ~500-fold stimulation of ADP-ribose polymer synthesis after PARP binding to the broken DNA ends (28) and *2*) numerous findings in cell culture and animal models of cardiovascular and neurodegenerative diseases, cancer, and inflammation as well as diabetes, suggesting that PARP activation is prevented or reversed by superoxide dismutase mimetics (26,29), hydroxyl radical scavengers (26,30), and peroxynitrite decomposition catalysts (3,28), as well as indirect antioxidants, i.e., aldose reductase inhibitors (11) or an-giotensin-2 converting enzyme inhibitors (31). However, as discussed in the introduction, recent findings in cell culture models of diabetes suggest that early high-glucose–induced PARP activation could be mediated via some unidentified metabolic mechanism, different from oxidative-nitrosative stress, and contribute to rather than result from reactive oxygen and nitrogen species generation. The present study reveals the major contribution of PARP activation to nitrotyrosine formation in peripheral nerve, superoxide, and nitrotyrosine formation in epineurial arterioles of vasa nervorum and superoxide production in aorta of STZ-induced diabetic rats. Similar interactions between PARP activity and superoxide, HNE adduct, and nitrosylated protein abundance have been observed in high-glucose–exposed HSC. Note that PARP-1 abundance was not affected by high glucose or ABA treatment, but ABA decreased high-glucose–induced poly(ADP-ribosy-l)ated protein overexpression. The latter is consistent with the current view on PARP-1 as abundantly expressed in most cell types with very minor, if any, transcriptional regulation (26).

A profound effect of the PARP inhibitor ABA on diabetes-associated oxidative-nitrosative stress, i.e., complete or essential correction of superoxide and nitrotyrosine production, cannot be attributed to weak antioxidant properties of the compound (32) for two major reasons. First, the antioxidant properties of ABA are related to its ability to act as a hydroxyl radical scavenger and thus preserve intracellular reduced glutathione (32,33). Such effect, observed with extremely high doses of the compound (500 mg $\cdot$ kg^{-1} $\cdot$ day^{-1} i.p., i.e., >16-fold higher than in the present study, [33]), should lead to neuralization of hydrogen peroxide and prevent formation of lipid peroxide without any impact on superoxide formation. Superoxide is the source, but not the product, of hydrogen peroxide or hydroxyl radicals, and benzamides and related compounds (e.g., nicotinamide) do have superoxide anion radical scavenging properties. Second, similar effects of PARP inhibition on superoxide in aorta, superoxide and nitrotyrosine in vasa nervorum, and nitrosylated protein abundance in high-glucose–exposed

HSC were also observed in our recent studies (34) with another PARP inhibitor 1,5-isoquinolinediol employed at 10-fold (in vivo) and 250-fold (in vitro) lower doses than ABA. Such doses are unlikely to cause any direct antioxidant effects. Note that ABA's effect on HNE adduct abundance, i.e., variable of lipid peroxidation can be attributed to both direct antioxidant properties of the compound and its independent effects on superoxide and nitrotyrosine formation.

PARP activation can contribute to diabetes-induced superoxide anion radical formation via multiple mechanisms. On the one hand, diabetes-associated decrease of peripheral nerve free mitochondrial and cytosolic NAD^+-to-NADH ratios is PARP-mediated and is reversed by a PARP inhibitor (35). Therefore, PARP activation is likely to upregulate activities of both extramitochondrial NAD(P)H oxidase and mitochondrial NADH oxidase, the important superoxide-generating enzymes. Poly(ADP-ribosyl)ation of glyceraldehyde 3-phosphate dehydrogenase, if present, may lead to protein kinase C activation and advanced glycation end product formation (19), both known to contribute to superoxide anion radical generation via protein kinase C–dependent activation of NAD(P)H oxidase (36), Maillard reaction (37), and advanced glycation end product interactions with their receptors (38), as well as glycation and downregulation of antioxidative defense enzymes (39). Thus, PARP activation may be involved in superoxide generation via multiple metabolic mechanisms. On the other hand, PARP activation alters transcriptional regulation and activates nuclear factor-κB, activator protein-1, signal transducer and activator of transcription-1, and others (18). Such activation leads to increased formation of endothelin-1 (21) and inflammatory cytokines, i.e., tumor necrosis factor-α, interleukin-6, and interleukin-$1\beta_1$, all known to contribute to superoxide generation (40,41). In addition, PARP activation results in poly(ADP-ribosyl)ation of numerous mitochondrial proteins (42), and the impact of this phenomenon on mitochondrial superoxide production remains to be explored.

Our finding of markedly reduced nitrotyrosine immunoreactivities in ABA-treated diabetic rats compared with the untreated diabetic group suggests that PARP activation is an important contributor to nitrosative stress in peripheral nerve and vasa nervorum in the STZ-induced diabetic rat model. Furthermore, quantitatively identical high-glucose–induced accumulation of nitrosylated (2.3-fold) and poly-(ADP-ribosyl)ated (1.8-fold) proteins in HSC and its complete or almost complete prevention by ABA treatment indicates that a similar mechanism operates in early human PDN. Nitrotyrosine is a footprint of peroxynitrite, a potent oxidant produced in the superoxide anion radical reaction with nitric oxide. Any approach counteracting superoxide formation, including PARP inhibition, will decrease peroxynitrite generation and nitrosylated protein abundance. It is important to remember that PARP activation leads to nuclear factor-κB–mediated upregulation of the iNOS gene (18). iNOS is the main donor of nitric oxide for peroxynitrite formation in tissue sites for diabetes complications (45,46). iNOS expression was increased in HSC cultured in 30 mmol/l glucose, compared with those cultured in 5.5 mmol/l glucose, and this increase was prevented by a PARP inhibitor treatment. Thus, PARP inhibition counteracts nitrosative stress via arrest of both superoxide and nitric oxide formation.

In addition to superoxide anion radicals and peroxynitrite, PARP activation may contribute to other free radical and oxidant formation in tissue sites for diabetes complications. It is reasonable to expect that by upregulating cyclooxygenase-2 (18) and promoting glutamate accumulation (36), PARP activation leads to increased production of hydroxyl radicals and hydrogen peroxide as well as lipid peroxidation (45,46). The effect of ABA on HNE adduct abundance in high-glucose–exposed HSC in our study may be at least partially mediated via inhibition of COX-2 protein expression. The consequences of PARP activation in diabetic tissues cannot be completely understood without identification of poly (ADP-ribosyl)ated transcription factors and other extramitochondrial and intramitochondrial proteins, as well as

PARP-regulated genes that encode factors involved in oxidant generation and antioxidative defense. Note that PARP activation contributes to Erk1/2 and *p*-38 mitogen-activated protein kinase phosphorylation as well as inhibition of phosphatidyl inositol 3′-kinase/Akt pathway (47), which makes the relations among oxidative-nitrosative stress, PARP activation, and a variety of metabolic and signaling pathways that can indirectly affect both oxidative stress and PARP even more complex.

In conclusion, PARP activation leads to oxidative-nitrosative stress in experimental PDN and high-glucose–exposed HSC. This probably occurs via multiple metabolic pathways and changes in gene expression. A complete understanding of the complex relations between oxidative-nitrosative stress and PARP activation in diabetes may require cutting-edge technologies such as genomics and proteomics.

Acknowledgements

The study was supported by an American Diabetes Association Research Grant (to I.G.O.), National Institutes of Health Grant DK59809-01 (to I.G.O.), Juvenile Diabetes Research Foundation International Grant (to I.G.O.), Juvenile Diabetes Research Foundation Center for the Study of Complications of Diabetes Grant 4-200-421 (to I.G.O. and M.J.S.), National Institutes of Health Grant DK 058005-04 (to M.A.Y.), and the Intramural Research Program of the National Institutes of Health, National Institute of Alcohol Abuse and Aging (to P.P.).

Glossary

ABA
: 3-aminobenzamide

HNE
: hydroxynonenal

HSC
: human Schwann cells

iNOS
: inducible nitric oxide synthase

NAD^+
: nicotinamide adenine dinucleotide

PARP
: poly(ADP-ribose) polymerase

PDN
: peripheral diabetic neuropathy

STZ
: streptozocin

References

1. Coppey LJ, Gellett JS, Davidson EP, Dunlap JA, Lund DD, Yorek MA. Effect of antioxidant treatment of streptozotocin-induced diabetic rats on endoneurial blood flow, motor nerve conduction velocity, and vascular reactivity of epineurial arterioles of the sciatic nerve. Diabetes 2001;50:1927–1937. [PubMed: 11473057]
2. Cameron NE, Tuck Z, McCabe L, Cotter MA. Effect of the hydroxyl radical scavenger, dimethylthiourea, on peripheral nerve tissue perfusion, conduction velocity and nociception in experimental diabetes. Diabetologia 2001;44:1161–1169. [PubMed: 11596672]

3. Obrosova IG, Mabley JG, Zsengeller Z, Charniauskaya T, Abatan OI, Groves JT, Szabo C. Role for nitrosative stress in diabetic neuropathy: evidence from studies with a peroxynitrite decomposition catalyst. FASEB J 2005;19:401–403. [PubMed: 15611153]
4. Stevens MJ, Obrosova I, Cao X, Van Huysen C, Greene DA. Effects of DL-alpha-lipoic acid on peripheral nerve conduction, blood flow, energy metabolism, and oxidative stress in experimental diabetic neuropathy. Diabetes 2000;49:1006–1015. [PubMed: 10866054]
5. Hounsom L, Corder R, Patel J, Tomlinson DR. Oxidative stress participates in the breakdown of neuronal phenotype in experimental diabetic neuropathy. Diabetologia 2001;44:424–428. [PubMed: 11357471]
6. Ametov AS, Barinov A, Dyck PJ, Hermann R, Kozlova N, Litchy WJ, Low PA, Nehrdich D, Novosadova M, O'Brien PC, Reljanovic M, Samigullin R, Schuette K, Strokov I, Tritschler HJ, Wessel K, Yakhno N, Ziegler D. the SYDNEY Trial Study Group. The sensory symptoms of diabetic polyneuropathy are improved with agr;-lipoic acid: the SYDNEY trial. Diabetes Care 2003;26:770–776. [PubMed: 12610036]
7. Li F, Obrosova IG, Abatan O, Tian D, Larkin D, Stuenkel EL, Stevens MJ. Taurine replacement attenuates hyperalgesia and abnormal calcium signaling in sensory neurons of streptozotocin-diabetic rats. Am J Physiol Endocrinol Metab 2005;288:E29–E36. [PubMed: 15585600]
8. Sagara M, Satoh J, Wada R, Yagihashi S, Takahashi K, Fukuzawa M, Muto G, Muto Y, Toyota T. Inhibition of development of peripheral neuropathy in streptozotocin-induced diabetic rats with N-acetylcysteine. Diabetologia 1996;39:263–269. [PubMed: 8721770]
9. Schmeichel AM, Schmelzer JD, Low PA. Oxidative injury and apoptosis of dorsal root ganglion neurons in chronic experimental diabetic neuropathy. Diabetes 2003;52:165–171. [PubMed: 12502508]
10. Cheng C, Zochodne DW. Sensory neurons with activated caspase-3 survive long-term experimental diabetes. Diabetes 2003;52:2363–2371. [PubMed: 12941777]
11. Obrosova IG, Pacher P, Szabo C, Zsengeller Z, Hirooka H, Stevens MJ, Yorek MA. Aldose reductase inhibition counteracts oxidative-nitrosative stress and poly(ADP-ribose) polymerase activation in tissue sites for diabetes complications. Diabetes 2005;54:234–242. [PubMed: 15616034]
12. Stevens MJ, Zhang W, Li F, Sima AA. C-peptide corrects endoneurial blood flow but not oxidative stress in type 1 BB/Wor rats. Am J Physiol Endocrinol Metab 2004;287:E497–E505. [PubMed: 15126237]
13. Oltman CL, Coppey LJ, Gellett JS, Davidson EP, Lund DD, Yorek MA. Progression of vascular and neural dysfunction in sciatic nerves of zucker diabetic fatty (ZDF) and zucker rats. Am J Physiol Endocrinol Metab 2005;289:E113–E122. [PubMed: 15727946]
14. Purves T, Middlemas A, Agthong S, Jude EB, Boulton AJ, Fernyhough P, Tomlinson DR. A role for mitogen-activated protein kinases in the etiology of diabetic neuropathy. FASEB J 2001;15:2508–2514. [PubMed: 11689477]
15. Pop-Busui R, Marinescu V, Van Huysen C, Li F, Sullivan K, Greene DA, Larkin D, Stevens MJ. Dissection of metabolic, vascular, and nerve conduction interrelationships in experimental diabetic neuropathy by cyclooxygenase inhibition and acetyl-L-carnitine administration. Diabetes 2002;51:2619–2628. [PubMed: 12145179]
16. Garcia Soriano F, Virag L, Jagtap P, Szabo E, Mabley JG, Liaudet L, Marton A, Hoyt DG, Murthy KG, Salzman AL, Southan GJ, Szabo C. Diabetic endothelial dysfunction: the role of poly(ADP-ribose) polymerase activation. Nat Med 2001;7:108–113. [PubMed: 11135624]
17. Obrosova IG, Li F, Abatan OI, Forsell MA, Komjati K, Pacher P, Szabo C, Stevens MJ. Role of poly (ADP-ribose) polymerase activation in diabetic neuropathy. Diabetes 2004;53:711–720. [PubMed: 14988256]
18. Ha HC, Hester LD, Snyder SH. Poly(ADP-ribose) polymerase-1 dependence of stress-induced transcription factors and associated gene expression in glia. Proc Natl Acad Sci U S A 2002;99:3270–3275. [PubMed: 11854472]
19. Du X, Matsumura T, Edelstein D, Rossetti L, Zsengeller Z, Szabo C, Brownlee M. Inhibition of GAPDH activity by poly(ADP-ribose) polymerase activates three major pathways of hyperglycemic damage in endothelial cells. J Clin Invest 2003;112:1049–1057. [PubMed: 14523042]

20. Pacher P, Liaudet L, Soriano FG, Mabley JG, Szabo E, Szabo C. The role of poly(ADP-ribose) polymerase activation in the development of myocardial and endothelial dysfunction in diabetes. Diabetes 2002;51:514–521. [PubMed: 11812763]
21. Minchenko AG, Stevens MJ, White L, Abatan OI, Komjati K, Pacher P, Szabo C, Obrosova IG. Diabetes-induced overexpression of endothelin-1 and endothelin receptors in the rat renal cortex is mediated via poly(ADP-ribose) polymerase activation. FASEB J 2003;17:1514–1516. [PubMed: 12824290]
22. Zheng L, Szabo C, Kern TS. Poly(ADP-Ribose) polymerase is involved in the development of diabetic retinopathy via regulation of nuclear factor-κB. Diabetes 2004;53:2960–2967. [PubMed: 15504977]
23. Li F, Drel VR, Szabo C, Stevens MJ, Obrosova IG. Low-dose poly(ADP-ribose) polymerase inhibitor-containing combination therapies reverse early peripheral diabetic neuropathy. Diabetes 2005;54:1514–1522. [PubMed: 15855340]
24. Obrosova IG, Fathallah L, Lang HJ, Greene DA. Evaluation of a sorbitol dehydrogenase inhibitor on diabetic peripheral nerve metabolism: a prevention study. Diabetologia 1999;42:1187–1194. [PubMed: 10525658]
25. Towbin H, Staehelin T, Gordon J. Electrophoretic transfer of proteins from polyacrylamide gels to nitrocellulose sheets: Procedure and some applications 1979. Biotechnology 1992;24:145–149. [PubMed: 1422008]
26. Virag L, Szabo C. The therapeutic potential of poly(ADP-ribose) polymerase inhibitors. Pharmacol Rev 2002;54:375–429. [PubMed: 12223530]
27. Soldatenkov VA, Potaman VN. DNA-binding properties of poly(ADP-ribose) polymerase: a target for anticancer therapy. Curr Drug Targets 2004;5:357–365. [PubMed: 15134218]
28. Alvarez-Gonzalez R, Pacheco-Rodriguez G, Mendoza-Alvarez H. Enzymology of ADP-ribose polymer synthesis. Mol Cell Biochem 1994;138:33–37. [PubMed: 7898472]
29. Cuzzocrea S, Genovese T, Mazzon E, Di Paola R, Muia C, Britti D, Salvemini D. Reduction in the development of cerulein-induced acute pancreatitis by treatment with M40401, a new selective superoxide dismutase mimetic. Shock 2004;22:254–261. [PubMed: 15316396]
30. Zingarelli B, Scott GS, Hake P, Salzman AL, Szabo C. Effects of nicaraven on nitric oxide-related pathways and in shock and inflammation. Shock 2000;13:126–134. [PubMed: 10670842]
31. Szabo C, Pacher P, Zsengeller Z, Vaslin A, Komjati K, Benko R, Chen M, Mabley JG, Kollai M. Angiotensin II-mediated endothelial dysfunction: role of poly(ADP-ribose) polymerase activation. Mol Med 2004;10:28–35. [PubMed: 15502880]
32. Wilson GL, Patton NJ, McCord JM, Mullins DW, Mossman BT. Mechanisms of streptozotocin- and alloxan-induced damage in rat B cells. Diabetologia 1984;27:587–291. [PubMed: 6241574]
33. Cover C, Fickert P, Knight TR, Fuchsbichler A, Farhood A, Trauner M, Jaeschke H. Pathophysiological role of poly(ADP-ribose) polymerase (PARP) activation during acetaminophen-induced liver cell necrosis in mice. Toxicol Sci 2005;84:201–208. [PubMed: 15601672]
34. Obrosova IG, Drel VR, Pacher P, Stevens MJ, Yorek MA. Oxidative stress—poly(ADP-ribose) polymerase activation: the relation is revisited (Abstract). Diabetes 2005;54 (Suppl 1):A213.
35. Li F, Szabo C, Pacher P, Southan GJ, Abatan OI, Charniauskaya T, Stevens MJ, Obrosova IG. Evaluation of orally active poly(ADP-ribose) polymerase inhibitor in streptozotocin-diabetic rat model of early peripheral neuropathy. Diabetologia 2004;47:710–717. [PubMed: 15298348]
36. Inoguchi T, Sonta T, Tsubouchi H, Etoh T, Kakimoto M, Sonoda N, Sato N, Sekiguchi N, Kobayashi K, Sumimoto H, Utsumi H, Nawata H. Protein kinase C-dependent increase in reactive oxygen species (ROS) production in vascular tissues of diabetes: role of vascular NAD(P)H oxidase. J Am Soc Nephrol 2003;14 (Suppl 3):S227–S232. [PubMed: 12874436]
37. Ukeda H, Shimamura T, Tsubouchi M, Harada Y, Nakai Y, Sawamura M. Spectrophotometric assay of superoxide anion formed in Maillard reaction based on highly water-soluble tetrazolium salt. Anal Sci 2002;18:1151–1154. [PubMed: 12400664]
38. Loske C, Neumann A, Cunningham AM, Nichol K, Schinzel R, Riederer P, Munch G. Cytotoxicity of advanced glycation endproducts is mediated by oxidative stress. J Neural Transm 1998;105:1005–1015. [PubMed: 9869332]
39. Thornalley PJ. Glycation in diabetic neuropathy: characteristics, consequences, causes, and therapeutic options. Int Rev Neurobiol 2002;50:37–57. [PubMed: 12198817]

40. Ergul A, Johansen JS, Stromhaug C, Harris AK, Hutchinson J, Tawfik A, Rahimi A, Rhim E, Wells B, Caldwell RW, Anstadt MP. Vascular dysfunction of venous bypass conduits is mediated by reactive oxygen species in diabetes: role of endothelin-1. J Pharmacol Exp Ther 2005;313:70–77. [PubMed: 15608082]

41. Busserolles J, Paya M, D'Auria MV, Gomez-Paloma L, Alcaraz MJ. Protection against 2,4,6-trinitrobenzenesulphonic acid-induced colonic inflammation in mice by the marine products bolinaquinone and petrosaspongiolide M. Biochem Pharmacol 2005;69:1433–1440. [PubMed: 15857607]

42. Lai YC, Chen Y, Zhang X, Kochanek PM, Nathaniel PD, Jenkins L, Clark RS, Szabo C. Poly-adpribosylation as a post-translational modification of mitochondrial proteins: 82 (Abstract). Crit Care Med 2004;32 (Suppl 12):A21.

43. Du Y, Smith MA, Miller CM, Kern TS. Diabetes-induced nitrative stress in the retina, and correction by aminoguanidine. J Neurochem 2002;80:771–779. [PubMed: 11948240]

44. Fan Q, Liao J, Kobayashi M, Yamashita M, Gu L, Gohda T, Suzuki Y, Wang LN, Horikoshi S, Tomino Y. Candesartan reduced advanced glycation end-products accumulation and diminished nitro-oxidative stress in type 2 diabetic KK/Ta mice. Nephrol Dial Transplant 2004;19:3012–3020. [PubMed: 15574998]

45. Lancelot E, Callebert J, Plotkine M, Boulu RG. Striatal dopamine participates in glutamate-induced hydroxyl radical generation.

46. Agha AM, El-Khatib AS, Al-Zuhair H. Modulation of oxidant status by meloxicam in experimentally induced arthritis. Pharmacol Res 1999;40:385–392. [PubMed: 10527652]

47. Veres B, Radnai B, Gallyas F Jr, Varbiro G, Berente Z, Osz E, Sumegi B. Regulation of kinase cascades and transcription factors by a poly(ADP-ribose) polymerase-1 inhibitor, 4-hydroxyquinazoline, in lipopolysaccharide-induced inflammation in mice. J Pharmacol Exp Ther 2004;310:247–255. [PubMed: 14999056]

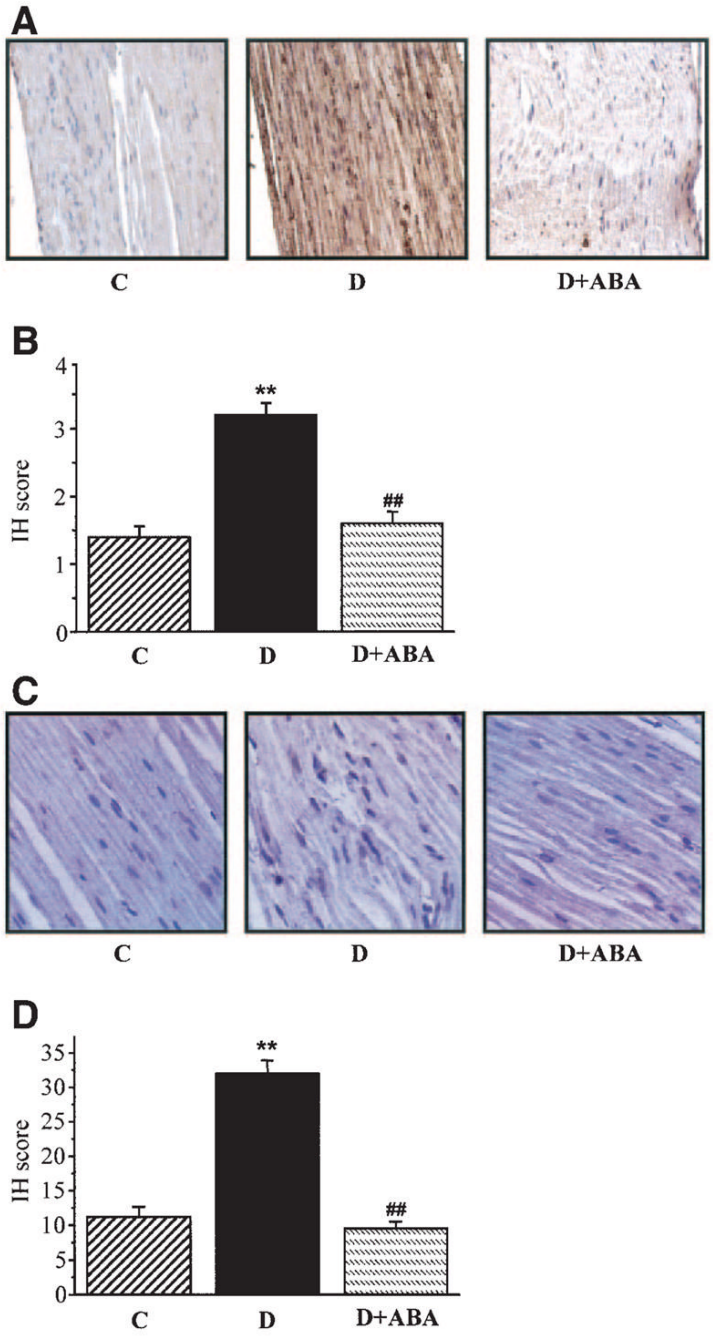

FIG. 1.

A: Representative microphotographs of immunohistochemical stainings of nitrotyrosine in sciatic nerves of control rats, diabetic rats, and diabetic rats treated with ABA. Magnification × 400. *B*: Immunohistochemistry scores (IH) of sciatic nerve nitrotyrosine stainings (mean ± SE). *C*: Representative microphotographs of immunohistochemical stainings of poly(ADP-ribose) in sciatic nerves of control rats, diabetic rats, and diabetic rats treated with ABA. Magnification × 400. *D*: Counts of poly(ADP-ribose)-positive nuclei in sciatic nerves of control rats, diabetic rats, and diabetic rats treated with ABA. In all figures, C, control; D, diabetes; D + ABA, diabetes + ABA. n = 10–18 per group.

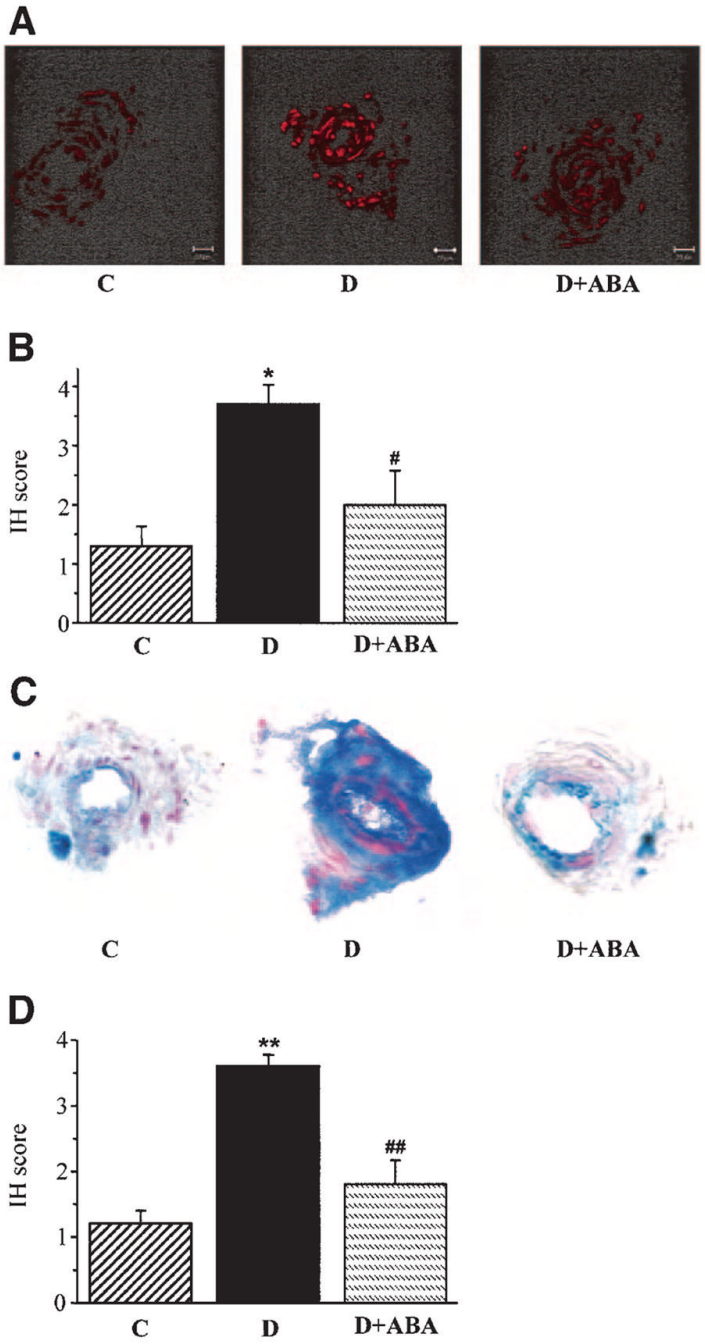

FIG. 2.

A: Representative microphotographs of superoxide-generated fluorescence in sciatic nerve epineurial vessels of control rats, diabetic rats, and diabetic rats treated with ABA. *n* = 3 per group. *B*: Scores of epineurial vessel superoxide-generated immunofluorescence (mean ± SE). *C*: Representative microphotographs of nitrotyrosine immunohistochemical staining in sciatic nerve epineurial vessels of control rats, diabetic rats, and diabetic rats treated with ABA. *n* = 5–8 per group. Magnification ×40. *D*: Immunohistochemistry scores (IH) of epineurial vessel nitrotyrosine stainings (mean ± SE). C, control; D, diabetes; D + ABA, diabetes + ABA.

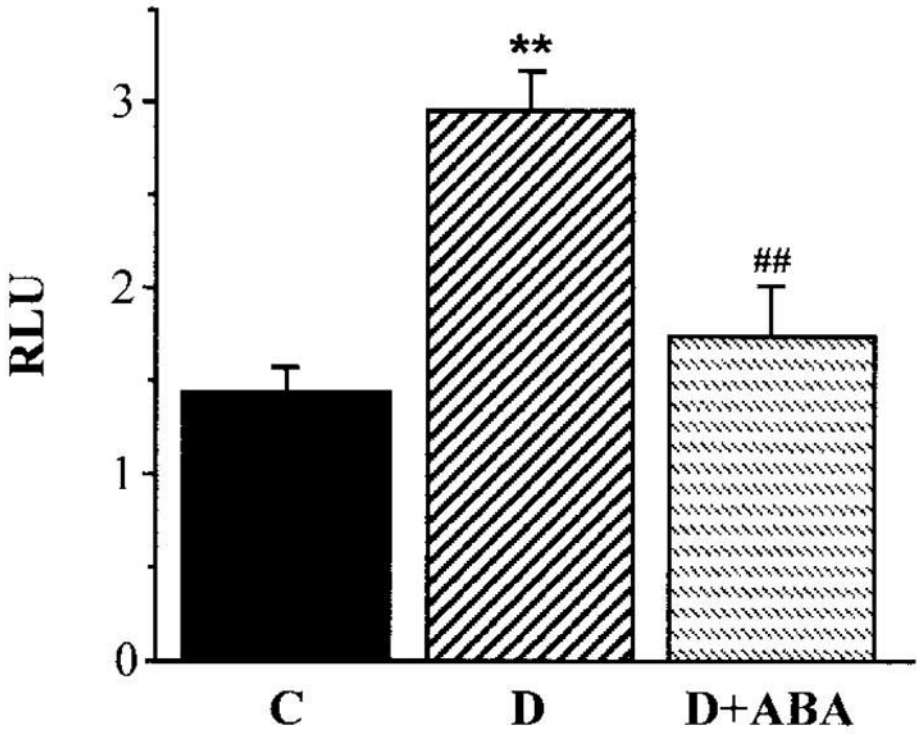

FIG. 3.

Superoxide anion radical luminescence in aortas of control rats, diabetic rats, and diabetic rats treated with ABA. *n* = 5–6 per group. C, control; D, diabetes; D + ABA, diabetes + ABA; RLU, relative luminescence units.

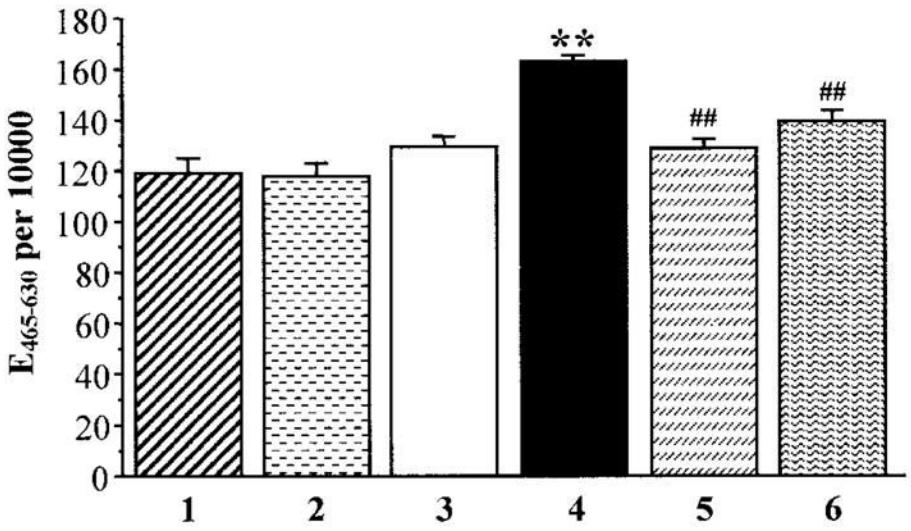

FIG. 4.

Superoxide-generated ethidium fluorescence in human Schwann cells cultured in 5.5 mmol/l glucose (*1*), 5.5 mmol/l glucose + 5 mmol/l ABA (*2*), 5.5 mmol/l glucose + 50 μmol/l Mn(III) TBAP (*3*), 30 mmol/l glucose (*4*), 30 mmol/l glucose + 5 mmol/l ABA (*5*), and 5.5 mmol/l glucose + 50 μmol/l Mn(III) TBAP (*6*). Mean ± SE, $n = 5$ per group. $^{**}P < 0.01$ vs. cells cultured in 5.5 mmol/l glucose; $^{\#\#}P < 0.01$ vs. cells cultured in 30 mmol/l glucose without additions of ABA or Mn(III) TBAP. UF, units of fluorescence.

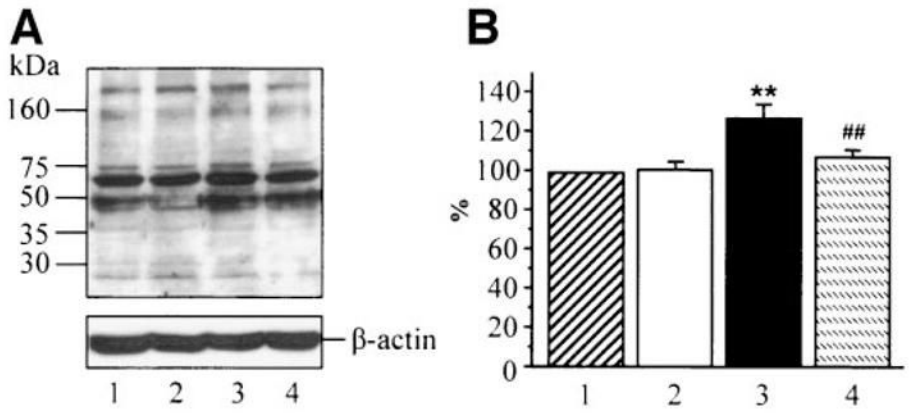

FIG. 5.

A: Representative Western blot analysis of HSC chemically reduced amino acid-(4)-hydroxynonenal adducts. Equal protein loading was confirmed with β-actin antibody. *Lane 1*: 5.5 mmol/l glucose; *lane 2*: 5.5 mmol/l glucose + ABA; *lane 3*: 30 mmol/l glucose; and *lane 4*: 30 mmol/l glucose + 5 mmol/l ABA. *B*: Chemically reduced amino acid-(4)-hydroxynonenal adduct content in HSC cultured in 5.5 mmol/l glucose (1), 5.5 mmol/l glucose + ABA (2), 30 mmol/l glucose (3), and 30 mmol/l glucose + ABA (4). Chemically reduced amino acid-(4)-hydroxynonenal adduct content in cells cultured in 5.5 mmol/l glucose is taken as 100%. Mean ± SE, $n = 5$ per group. $^{**}P < 0.01$ vs. cells cultured in 5.5 mmol/l glucose; $^{\#\#}P < 0.01$ vs. cells cultured in 30 mmol/l glucose without ABA.

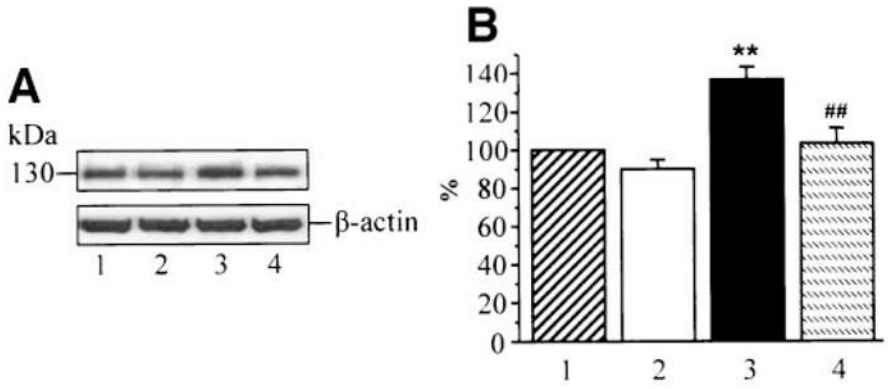

FIG. 6.

A: Representative Western blot analysis of HSC iNOS. Equal protein loading was confirmed with β-actin antibody. *Lane 1*: 5.5 mmol/l glucose; *lane 2*: 5.5 mmol/l glucose + ABA; *lane 3*: 30 mmol/l glucose; and *lane 4*: 30 mmol/l glucose + 5 mmol/l ABA. *B*: Inducible nitric oxide synthase protein content in HSC cultured in 5.5 mmol/l glucose (1), 5.5 mmol/l glucose + ABA (2), 30 mmol/l glucose (3), and 30 mmol/l glucose plus ABA (4). Total iNOS content in cells cultured in 5.5 mmol/l glucose is taken as 100%. Mean ± SE, $n = 5$ per group. $^{**}P < 0.01$ vs. cells cultured in 5.5 mmol/l glucose, $^{\#\#}P < 0.01$ vs. cells cultured in 30 mmol/l glucose without ABA.

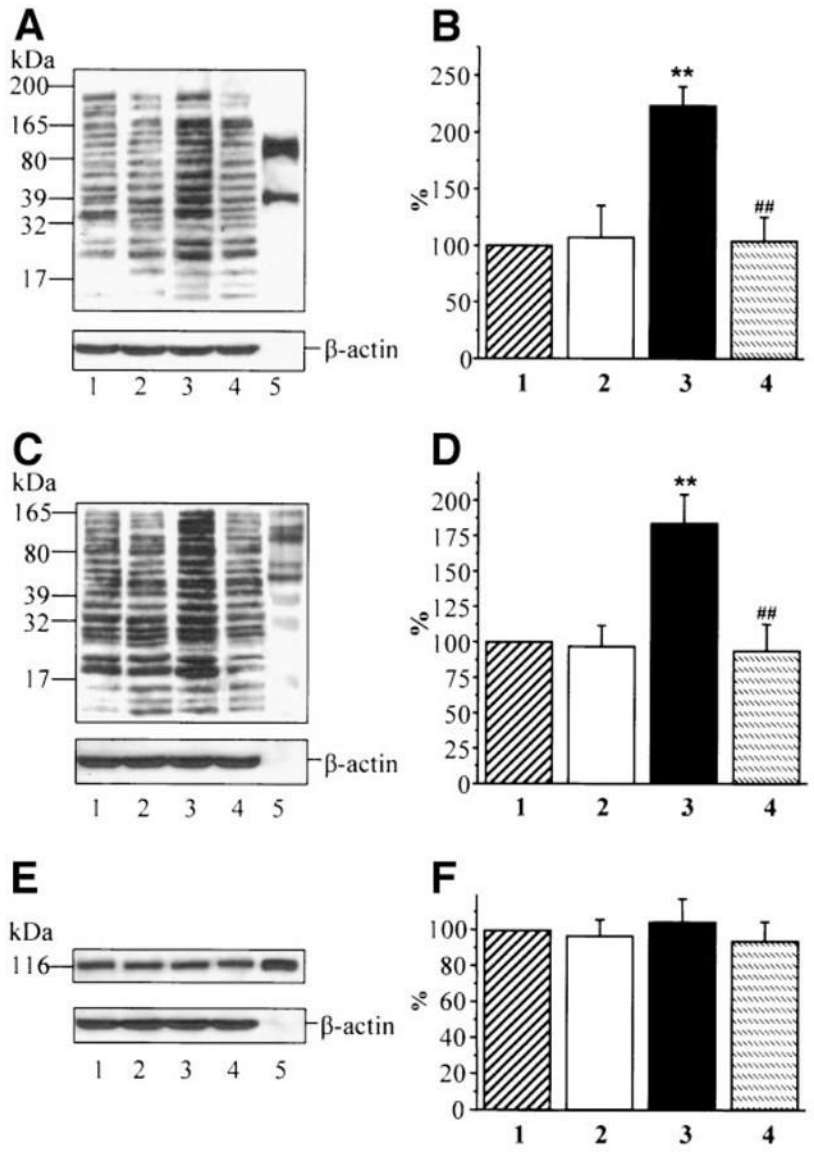

FIG. 7.

A: Representative Western blot analysis of HSC nitrosylated proteins. Equal protein loading was confirmed with β-actin antibody. *Lane 1*: 5.5 mmol/l glucose; *lane 2*: 5.5 mmol/l glucose + ABA; *lane 3*: 30 mmol/l glucose; *lane 4*: 30 mmol/l glucose + 5 mmol/l ABA; and *lane 5*: nitrotyrosine positive control. *B*: Total nitrosylated protein content in HSC cultured in 5.5 mmol/l glucose (1), 5.5 mmol/l glucose + ABA (2), 30 mmol/l glucose (3), and 30 mmol/l glucose plus ABA (4). Total nitrosylated protein content in cells cultured in 5.5 mmol/l glucose is taken as 100%. *C*: Representative Western blot analysis of HSC poly-(ADP-ribosyl)ated proteins. Equal protein loading was confirmed with β-actin antibody. *Lane 1*: 5.5 mmol/l glucose; *lane 2*: 5.5 mmol/l glucose + ABA; *lane 3*: 30 mmol/l glucose; *lane 4*: 30 mmol/l glucose + 5 mmol/l ABA; and *lane 5*: poly(ADP-ribosyl)ated protein positive control. *D*: Total poly(ADP-ribosyl)ated protein content in HSC cultured in 5.5 mmol/l glucose (1), 5.5 mmol/l glucose + ABA (2), 30 mmol/l glucose (3), and 30 mmol/l glucose + ABA (4). Total poly (ADP-ribosyl)ated protein content in cells cultured in 5.5 mmol/l glucose is taken as 100%. *E*: Representative Western blot analysis of HSC PARP-1 protein. Equal protein loading was

confirmed with β-actin antibody. *Lane 1*: 5.5 mmol/l glucose; *lane 2*: 5.5 mmol/l glucose + ABA; *lane 3*: 30 mmol/l glucose; *lane 4*: 30 mmol/l glucose + 5 mmol/l ABA; and *lane 5*: PARP-1 enzyme. *F*: Total PARP-1 protein content in HSC cultured in 5.5 mmol/l glucose (1), 5.5 mmol/l glucose + ABA (2), 30 mmol/l glucose (3), and 30 mmol/l glucose + ABA (4). Total PARP-1 protein content in cells cultured in 5.5 mmol/l glucose is taken as 100%. In *B*, *D*, and *F*, the results are expressed as mean ± SE, $n = 5$ per group. $^{**}P < 0.01$ vs. cells cultured in 5.5 mmol/l glucose; $^{\#\#}P < 0.01$ vs. cells cultured in 30 mmol/l glucose.

TABLE 1

Initial and final body weights and final blood glucose concentrations in control and diabetic rats with and without ABA treatment

	Body weight (g)		Blood glucose
	Initial*	Final	(mmol/l)
Control	279 ± 6	483 ± 9	4.98 ± 0.22
Diabetes	288 ± 5	375 ± 16†	19.8 ± 1.26†
Diabetes + ABA	282 ± 6	359 ± 22†	20.6 ± 1.62†

Data are means ± SE, n = 10–18.

*Before induction of STZ-induced diabetes.

†Significantly different from controls ($P < 0.01$).